A single amino acid substitution in CFTR converts ATP to an inhibitory ligand

Wen-Ying Lin,[1,2] Kang-Yang Jih,[2,3] and Tzyh-Chang Hwang[1,2]

[1]Department of Medical Pharmacology and Physiology, [2]Dalton Cardiovascular Research Center, University of Missouri–Columbia, Columbia, MO 65211

[3]Physician-Scientist Program, National Yang-Ming University, Taipei, 112 Taiwan

Cystic fibrosis (CF), one of the most common lethal genetic diseases, is caused by loss-of-function mutations of the cystic fibrosis transmembrane conductance regulator (CFTR) gene, which encodes a chloride channel that, when phosphorylated, is gated by ATP. The third most common pathogenic mutation, a glycine-to-aspartate mutation at position 551 or G551D, shows a significantly decreased open probability (P_o) caused by failure of the mutant channel to respond to ATP. Recently, a CFTR-targeted drug, VX-770 (Ivacaftor), which potentiates G551D-CFTR function in vitro by boosting its P_o, has been approved by the FDA to treat CF patients carrying this mutation. Here, we show that, in the presence of VX-770, G551D-CFTR becomes responsive to ATP, albeit with an unusual time course. In marked contrast to wild-type channels, which are stimulated by ATP, sudden removal of ATP in excised inside-out patches elicits an initial increase in macroscopic G551D-CFTR current followed by a slow decrease. Furthermore, decreasing [ATP] from 2 mM to 20 µM resulted in a paradoxical increase in G551D-CFTR current. These results suggest that the two ATP-binding sites in the G551D mutant mediate opposite effects on channel gating. We introduced mutations that specifically alter ATP-binding affinity in either nucleotide-binding domain (NBD1 or NBD2) into the G551D background and determined that this disease-associated mutation converts site 2, formed by the head subdomain of NBD2 and the tail subdomain of NBD1, into an inhibitory site, whereas site 1 remains stimulatory. G551E, but not G551K or G551S, exhibits a similar phenotype, indicating that electrostatic repulsion between the negatively charged side chain of aspartate and the γ-phosphate of ATP accounts for the observed mutational effects. Understanding the molecular mechanism of this gating defect lays a foundation for rational drug design for the treatment of CF.

The Journal of General Physiology

INTRODUCTION

Cystic fibrosis (CF), one of the most common lethal genetic diseases (Rowe et al., 2005), afflicts 1 in every ∼2,500 newborns in Caucasian populations (Zielenski and Tsui, 1995). The culprit behind CF is the malfunction of the CFTR protein, a chloride channel crucial to maintaining salt and water homeostasis across many epithelial tissues (Riordan et al., 1989; Quinton and Reddy, 1991; Bear et al., 1992). As a member of the ATP-binding cassette (ABC) protein superfamily, CFTR inherits the conserved structural motifs found in other ABC proteins: two nucleotide-binding domains (NBDs) using the energy in the form of ATP and two transmembrane domains (TMDs), which, in the case of CFTR, craft a gated chloride permeation pathway. In addition, CFTR is equipped with a unique regulatory (R) domain for PKA-dependent phosphorylation (Ostedgaard et al., 2001). It is generally held that after phosphorylation by PKA in the R domain, opening and closing of CFTR's gate in the TMDs are controlled by ATP-induced NBD dimerization and hydrolysis-triggered partial separation of the NBD dimer, respectively (Vergani et al., 2003, 2005; Hwang and Sheppard, 2009; Tsai et al., 2009, 2010). Mutations that disrupt normal gating could lead to CF. For example, converting the glycine residue at position 551 to an aspartate (i.e., G551D) results in a >100-fold lower open probability (P_o) compared with WT-CFTR (Bompadre et al., 2007; Miki et al., 2010). This third most common CF-associated mutation has drawn abundant attentions as finding reagents to raise its P_o (i.e., CFTR "potentiators") is expected to bear a major therapeutic impact on patients carrying such mutation.

Recent high-throughput drug screening has indeed yielded a high-affinity CFTR potentiator, VX-770 (Ivacaftor or Kalydeco [Van Goor et al., 2009]), which has soon become the first CFTR-targeted therapy. As shown to increase the P_o of G551D-CFTR by approximately eightfold in vitro (Van Goor et al., 2009), VX-770, when taken orally, significantly improves the symptoms of CF patients carrying such mutation (Accurso et al., 2010; Ramsey et al., 2011). Despite these encouraging results, the VX-770–rectified P_o of G551D channels is still less

Correspondence to Tzyh-Chang Hwang: hwangt@health.missouri.edu

Abbreviations used in this paper: ABC, ATP-binding cassette; CF, cystic fibrosis; NBD, nucleotide-binding domain; TMD, transmembrane domain.

The Rockefeller University Press $30.00
J. Gen. Physiol. Vol. 144 No. 4 311–320
www.jgp.org/cgi/doi/10.1085/jgp.201411247

than 1/10th of that of WT-CFTR (Jih and Hwang, 2013; but cf. Van Goor et al., 2009), an observation further corroborated by a recent in vivo study examining the effect of VX-770 on sweat secretion in patients taking the drug (Char et al., 2014). Therefore, elucidating the molecular mechanism underlying the gating defect of the G551D mutant may lay the foundation for designing second generation, more efficacious CFTR potentiators that may ultimately realize a cure for at least a subset of patients with CF.

Previous studies have demonstrated that the stimulatory effect of ATP is abolished by the G551D mutation despite a normal surface expression of the mutant proteins (Gregory et al., 1991; Li et al., 1996; Bompadre et al., 2007). Although it was speculated that the G-to-D mutation at position 551 likely impedes ATP-induced NBD dimerization because of the critical location of G551 (Lewis et al., 2004; Xu et al., 2014), the underlying mechanism for this gating defect has not been rigorously investigated partly because of the extremely low activity of the G551D channel (Bompadre et al., 2007). Structurally, the importance of G551, a conserved glycine in the so-called ABC protein signature sequence (LSGGQ; Fig. 1 A), is attested in the numerous crystal structures of the NBD dimer (Smith et al., 2002; Ren et al., 2004; Szentpétery et al., 2004a,b; Jones and George, 2007). For example, in the crystal structure of MJ0976 (Smith et al., 2002; Jones and George, 2007), a prototypical NBD dimer from *Methanocaldococcus jannaschii*, an extensive hydrogen bond network is seen between the ligand ATP and the signature sequence. Of particular note, the lack of a side chain at the equivalent position of G551 (i.e., G149 in MJ0976; Fig. 1 A) exposes the peptide backbone so that ATP's γ-phosphate can form a hydrogen bond with the backbone amide (Fig. 1 B). Thus, a missense mutation at this location may result in steric hindrance that interrupts ATP-induced NBD dimerization.

Here we showed that in the presence of VX-770, G551D-CFTR becomes responsive to ATP, albeit in a very strange way. Once the G551D-CFTR channels in excised inside-out patches are activated by PKA and ATP, upon ATP washout, the macroscopic current shows a biphasic time course: a rapid current increase followed by a slow decay (Fig. 1 C). This observation leads us to hypothesize that the G551D mutation converts one of the two ATP-binding sites into an inhibitory site. By manipulating ATP-binding affinities at either NBD, we provide evidence that ATP-binding site 2, defined as the one formed by the head subdomain of NBD2 and the tail subdomain of NBD1, assumes an inhibitory function upon ATP binding in G551D-CFTR. Because this inhibitory effect is observed also in G551E, but not in G551K or G551S, a basic chemical mechanism of an electrostatic repulsion between the negatively charged side chain of 551D/E and the γ-phosphate of ATP in shaping the observed mutational effects is proposed. Although the aforementioned conclusions are model independent, the experimental results will be discussed in the context of a kinetic scheme derived from a gating model proposed for WT-CFTR channels.

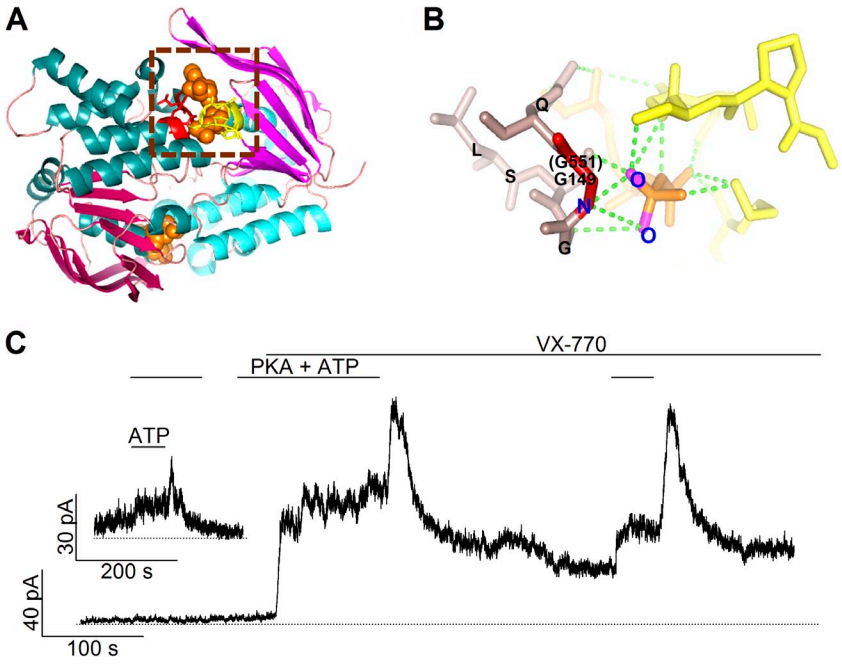

Figure 1. The roles of the conserved glycine at position 551 in the structure and function of CFTR. (A) The structure of a prototypical NBD dimer. A ribbon representation of the model was generated with PyMOL by using the dimeric MJ0796 NBD structure (PDB ID: 1L2T). The head and tail subdomains of each NBD are shown in magenta and cyan, respectively. Two ATP molecules, shown in a space-filling model, are sandwiched in the dimer interface. One of the signature sequences is shown in red, with the Walker A and B motifs of the partner NBD in yellow. (B) An expanded view of the part enclosed by the dashed square in A showing the hydrogen bond network between ATP and the signature sequence. The G149 residue (i.e., G551 in CFTR's NBD1) is highlighted in red, the rest of the signature sequence is in brown. ATP is presented in orange, and green dotted lines show possible hydrogen bonds. Parts of the Walker A and B motifs from the partner NBD are depicted in yellow. (C) A real-time current trace of G551D-CFTR channels showing an effect of VX-770 in potentiating the channel activity as well as a biphasic response of the current to ATP washout. The inset shows an experiment in which PKA was removed long before the addition and removal of ATP.

MATERIALS AND METHODS

Cell culture and transient expression system

Chinese hamster ovary (CHO) cells grown at 37°C in Dulbecco's modified Eagle's medium and supplemented with 10% fetal bovine serum were used for patch clamp experiments. Cells were transfected with pcDNA plasmids containing various CFTR constructs and pEGFP-C3 (Takara Bio Inc.) by using PolyFect (QIAGEN). The transfected CHO cells were cultured on sterile glass chips in 35-mm tissue dishes. We performed electrophysiological experiments 4–6 d after transfection.

Mutagenesis

For mutagenesis, QuikChange XL kit (Agilent Technologies) was used according to the manufacturer's protocols. To confirm the mutation made on cDNA, all of the DNA constructs were sequenced by the DNA core (University of Missouri).

Electrophysiological recordings

All of the electrophysiological experiments were performed at room temperature using an EPC9 amplifier (HEKA). Borosilicate capillary glasses were pulled into recording pipettes using a two-step micropipette puller (Narishige). The tip of micropipettes was polished using a homemade microforge before experiments. The resistance of polished pipettes was 1.5–3 MΩ in the bath solution. After observing the seal resistance >40 GΩ, we excised membrane patches into an inside-out mode and applied 2 mM ATP with 25 IU PKA to activate CFTR until the current reached a steady-state. The time course of this phosphorylation-dependent activation varies from patch to patch, but usually requires >5 min to reach the maximal level (e.g., see Fig. 2 A). To minimize effects of dephosphorylation by membrane-associated phosphatases and to assess the degree of phosphorylation-independent rundown, 10 IU PKA was added in all other ATP-containing solutions applied thereafter. To obtain macroscopic currents of G551D-CFTR for our kinetic studies, we applied 200 nM VX-770 in all experiments except the one shown in Fig. 3 C. For the macroscopic current recording, the membrane potential was kept at −30 mV, whereas single-channel recordings were made at −50 mV. The data were filtered with an eight-pole Bessel filter (LPF-8; Warner Instruments) with a 100-Hz cutoff frequency and digitized to a computer at a sampling rate of 500 Hz. For a better visual effect, we invert the inward current so that upward deflections represent channel openings. For recordings that demand fast solution changes, a perfusion system (SF-77B; Warner Instruments) with a dead time of ∼30 ms was used.

Chemicals and composition solutions

For all of the patches containing CFTR channels, the pipette solution contained (mM) 140 NMDG-Cl, 2 $MgCl_2$, 5 $CaCl_2$, and 10 HEPES, pH 7.4 with NMDG. Cells were perfused with a bath solution containing (mM) 145 NaCl, 5 KCl, 2 $MgCl_2$, 1 $CaCl_2$, 5 glucose, 5 HEPES, and 20 sucrose, pH 7.4 with NaOH. After establishing an inside-out configuration, we perfused the patch with a standard perfusion solution (i.e., intracellular solution) containing (mM) 150 NMDG-Cl, 2 $MgCl_2$, 10 EGTA, and 8 Tris, pH 7.4 with NMDG.

MgATP and PKA were purchased from Sigma-Aldrich. MgATP was stored in 500 mM stock solutions at −20°C prepared to working concentration, and the pH was adjusted to 7.4 with NMDG. VX-770, a gift from R. Bridges (Rosalind Franklin University, North Chicago, IL), was stored as a 100 µM stock in DMSO at −70°C and diluted to 200 nM.

Data analysis and statistics

The Igor Pro program (WaveMetrics) was used to measure the steady-state mean current amplitude. The current relaxation phase after ATP removal was fitted with single exponential functions in G551D- and G551D/W401G-CFTR and double exponential functions in WT-CFTR using a built-in Levenberg–Marquardt-based algorithm. Paired *t* test was conducted to compare the steady-state current in the presence of 20 µM ATP with that of 2 mM ATP (see Fig. 3), whereas two-tailed *t* test was used for comparing the relaxation time constants upon ATP washout in different constructs (see Fig. 5). All values are presented as mean ± SEM. The dwell time of each opening event in Fig. 7 was measured manually. Once the current stayed above the half amplitude threshold for 6 ms (four data points), they were counted as real openings; otherwise they were considered as noises. Because of the limited bandwidth of recordings as well as the small signal-to-noise ratio for G551D-CFTR, events shorter than 10 ms (four data points above the half amplitude threshold plus one data point before and one after, for a total of six data points with a 10-ms duration) cannot be measured accurately, resulting in missed events that may contribute partly to the apparent paucity of brief events in the dwell-time histograms shown in Fig. 7 (B and D).

We took a more conservative approach to analyze the single-channel open time for G551D and G551D/Y1219G channels as only current traces with up to two opening steps were used. When the events did contain overlapping openings, two kinds of measurement were taken. The first method counted the event as one channel opens for very long time until the end of the event and the other channel opens more briefly (i.e., an open duration representing only the overlapped open/close event). The second method measured the open time by assuming that the channel that opens first also closes first. Therefore, the first method would give more weight on the long opening events, whereas the second method underestimated the duration of long opening events. Fig. 7 shows open time histograms generated from numbers collected by the second method to provide a somewhat underestimated time constant for the long opening events.

RESULTS

As shown in Fig. 1 A, the glycine residue at the equivalent position of 551 plays a key role in ATP-induced dimerization of NBDs for ABC proteins. Thus, it seems unsurprising that previous studies show that ATP fails to increase the activity of G551D-CFTR in excised inside-out patches (Bompadre et al., 2007; Miki et al., 2010). Unexpectedly however, in the presence of VX-770, removal of ATP resulted in a sudden increase of the G551D-CFTR current followed by a slow decay (Figs. 1 C and 2 A). For technical reasons (see Materials and methods), we added PKA in all ATP-containing solutions, and thus PKA was also removed simultaneously upon washout of ATP. However, even in a few experiments in which PKA was only used for the initial phosphorylation-dependent activation, removal of ATP alone also caused a biphasic current change (Fig. 1 C, inset), indicating that phosphorylation/dephosphorylation does not account for the observed effects. This biphasic response to ATP removal is in stark contrast to the behavior of WT-CFTR (Fig. 2 B). Upon withdrawal of ATP for WT-CFTR channels, we observed a current decay with a time course that can be better described by a double exponential function (Fig. 2 B, red line): a fast phase that constitutes the major component of the current decay with a time constant <1 s and a minor but distinct slow phase with a

time constant of 29.6 ± 1.8 s (n = 8). Interestingly, this long time constant is indistinguishable from the time constant of the current decay seen with the G551D channels (31.1 ± 5.3 s; n = 12; Fig. 2 A, red line). It is also noted that the slow phase of current decay seen in WT currents is not caused by a small fraction of the channels being locked into a prolonged open state, a phenotype characteristic of hydrolysis-deficient CFTR mutants (Jih and Hwang, 2012), because clear opening and closing events are readily discernable in patches containing fewer channels (e.g., Fig. 2 C). We interpret this biphasic current relaxation as collected gating events reflecting the dissociation of ATP (or its hydrolytic products) from two distinct sites. The major difference between WT- and G551D-CFTR is that one normally stimulatory action of ATP is reversed in G551D channels, whereas the other one remains relatively unchanged.

The biphasic response upon ATP removal presented in Fig. 2 can thus be explained by a simple idea that the G551D mutation converts one of the stimulatory sites of ATP to an inhibitory site. Two predictions can be made based on this hypothesis. First, a decrease of [ATP] may first increase the G551D-CFTR current as the result of a lowered probability of occupancy for this presumed inhibitory site, but further lowering [ATP] will dampen the current as ATP binding to the stimulatory site is jeopardized. Second, mutations that alter ATP-binding affinities at the responsible ATP-binding site may differentially perturb the inhibitory or stimulatory action of ATP on G551D-CFTR. A simple way to test the first prediction is to measure G551D-CFTR currents at different [ATP]. Although we do not know a priori ATP affinities of these two binding sites, several clues may guide us to roughly estimate their sensitivity to ATP. First, as shown in Fig. 1 C, upon ATP washout, a rapid current rising, which represents dissociation of ATP from the inhibitory site, occurs before the slower current decay phase. This result indicates that the inhibitory site is of low affinity compared with the stimulatory site. Previous studies on WT-CFTR gating generally agreed that the catalysis-competent site 2 (composed of the head subdomain of NBD2 and the tail subdomain of NBD1) assumes a lower ATP-binding affinity than site 1 with an apparent K_d around 50–100 µM (Vergani et al., 2003; Bompadre et al., 2005; Zhou et al., 2006). In contrast, site 1 is hydrolysis incompetent (Stratford et al., 2007), and early biochemical studies show that ATP can be trapped in site 1 for minutes (Szabó et al., 1999; Aleksandrov et al., 2001, 2002; Basso et al., 2003), implicating a higher binding affinity for ATP. Recently, our functional studies using two independent approaches suggest that the lifetime of ATP bound to site 1 is around 30 s (Tsai et al., 2009, 2010), which is similar to the time constant of the slow current decay shown in Fig. 2 (A and B).

We therefore chose to test two more [ATP] values on G551D-CFTR in addition to 2 mM that is likely to saturate both ATP-binding sites: 20 µM, which presumably allows a full occupancy at site 1 but suboptimal binding of ATP to site 2, and 1 µM, which may ensure minimal binding of ATP to both sites. Results shown in Fig. 3 (A and B) indeed confirm our prediction: the G551D-CFTR current is increased when [ATP] is decreased from 2 mM to 20 µM (Fig. 3 A). However, a further decrease of [ATP] to 1 µM lowered the current (Fig. 3 B).

As all the results shown so far were conducted in the presence of VX-770, we have to ask whether this inhibitory action of ATP is also seen with G551D-CFTR in the absence of VX-770. It is technically challenging to conduct similar experiments in the absence of VX-770 because the open probability of G551D-CFTR is too low (Bompadre et al., 2007; Miki et al., 2010) to acquire patches yielding macroscopic currents. Once we are limited to small G551D-CFTR currents (<5 pA) in the absence of VX-770, a large current fluctuation caused by a

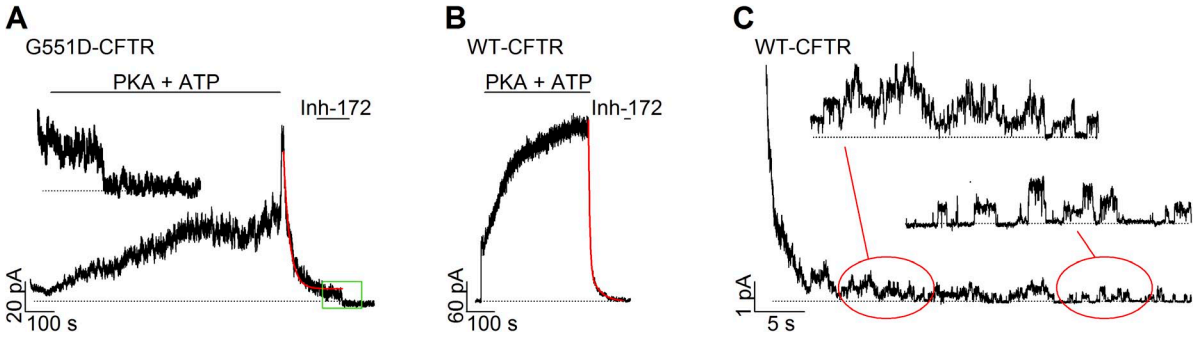

Figure 2. The G551D mutation alters the time course of current decay upon washout of ATP. (A and B) Biphasic changes of macroscopic currents upon ATP removal in the presence of VX-770 for G551D-CFTR (A) and WT-CFTR (B). (A) In the continuous presence of VX-770, addition of PKA and ATP slowly activated macroscopic G551D-CFTR currents to a steady-state. Subsequent removal of PKA and ATP results in a biphasic change of the current. The red line represents curve fit using a single exponential function. The inset shows expanded time course of current decrease upon the addition of Inh-172 (green box). (B) A real-time current trace showing different results with WT-CFTR under the same experimental protocol as in A. The red line marks curve fit using a double exponential function. (C) The current decay phase upon ATP removal in a patch containing fewer WT-CFTR. The red-circled areas are expanded as indicated.

huge number of channels in the patch would preclude ascertaining an unequivocal biphasic current change upon ATP removal. Nonetheless, we were able to reproduce the reverse [ATP] dependence of G551D-CFTR currents in the absence of VX-770 (Fig. 3 C), suggesting that the inhibitory action of ATP on site 2 is an intrinsic property of the G551D mutation. Interestingly however, the magnitude of current increase upon switching [ATP] from 2 mM to 20 µM is slightly enhanced by VX-770 (1.66 ± 0.14-fold, $n = 5$ with VX-770; and 1.34 ± 0.11-fold, $n = 8$ in the absence of VX-770; Fig. 3 D).

To further test the hypothesis that in G551D-CFTR site 2 becomes inhibitory, we manipulated ATP-binding affinity at site 2 by altering the aromatic amino acid Y1219 that has been shown both structurally and functionally (Zhou et al., 2006; PDG ID of NBD2: 3GD7) to play a pivotal role in ATP binding in the head subdomain of NBD2. Y1219F, Y1219I, and Y1219G, mutations known to cause a graded change of the apparent affinity for ATP (Zhou et al., 2006), were introduced into the G551D background. As predicted, mutating Y1219 to more conserved amino acids, such as phenylalanine and isoleucine, preserved the biphasic change in current amplitude, but with a noticeable smaller ratio of the peak current upon ATP washout to the steady-state current amplitude before washout (Fig. 4, A, B, and D). Also consistent with our hypothesis, removing the entire side chain, i.e., the G551D/Y1219G mutation, completely obliterates the rapid current increasing phase (Fig. 4 C) upon ATP removal as if only minimal occupancy of site 2 takes place at 2 mM [ATP]. These graded changes in the inhibitory action of ATP on G551D mutants echo the reported graded changes in ATP-binding affinity for the stimulatory action of ATP on WT-CFTR (Zhou et al., 2006). Thus, site 2, the main gating site for WT-CFTR, becomes inhibitory in G551D-CFTR! That the slow decay phase upon ATP removal is caused by ATP dissociation from site 1 is supported by the observation

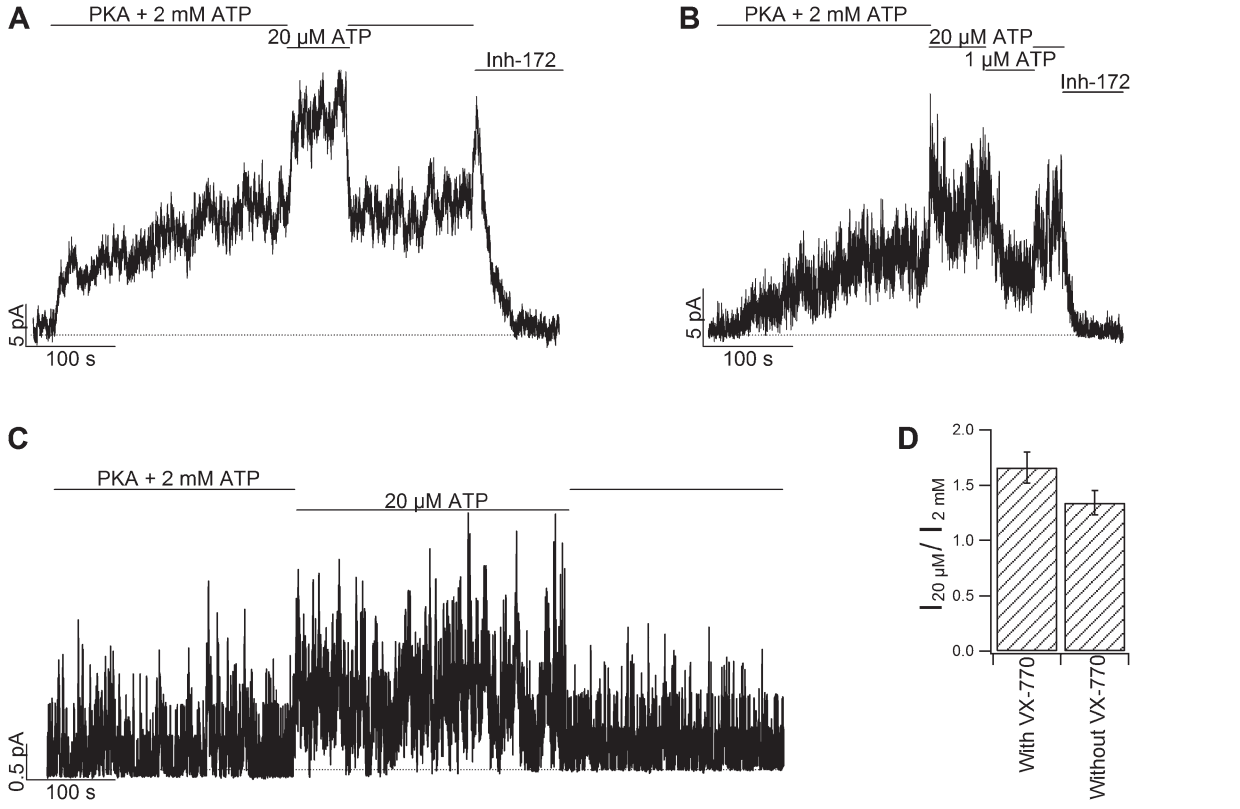

Figure 3. Paradoxical [ATP] dependence of G551D-CFTR currents supports the hypothesis of two ATP-binding sites exerting opposite actions. (A) Reversed ATP-dose dependence in G551D-CFTR. A switch from 2 mM to 20 µM ATP increased the current of G551D-CFTR, and the effect readily reversed once the ATP concentration was increased. The current in the presence of 20 µM ATP was 1.66-fold higher compared with that of 2 mM ATP ($P < 0.05$; paired t test). The current can be inhibited by a specific CFTR inhibitor, Inh-172 (Kopeikin et al., 2010). Note a biphasic current change is also seen when ATP removal takes place concurrently with the addition of Inh-172. This is likely because of a fast relief of ATP-dependent inhibition but a slow onset of current inhibition by Inh-172. Of note, an additional kinetic step is required after binding of Inh-172 to inhibit CFTR gating (Kopeikin et al., 2010). (B) A continuous recording of G551D-CFTR showing bell-shaped [ATP] dependence. Note a current increase when [ATP] is decreased from 2 mM to 20 µM, but a decrease of the current when [ATP] is further reduced to 1 µM. (C) Inverse [ATP] dependence of G551D-CFTR currents in the absence of VX-770. Note a reversible increase of the current upon switching [ATP] from 2 mM to 20 µM. The current in the presence of 20 µM ATP was 1.34-fold higher than that of 2 mM ATP ($P < 0.05$, paired t test). (D) Fold increase of G551D-CFTR currents upon switching solution from 2 mM to 20 µM ATP ($I_{20\mu M}/I_{2mM}$) in the presence or absence of VX-770. Mean ± SEM is shown.

that the time course of this current decrease is accelerated by mutating the equivalent aromatic amino acid, W401, in the head subdomain of NBD1 (Fig. 5 A). Of note, the time constant of slow current decay phase in G551D/Y1219G-CFTR was unchanged compared with G551D-CFTR (Figs. 4 C and 5 B), indicating that this slow current decay is not controlled by ATP dissociation from site 2.

As the lack of a side chain at position 551 exposes the peptide backbone so that a hydrogen bond can be formed between the γ-phosphate of ATP and the backbone amide upon NBD dimerization (Lewis et al., 2004), we reckoned that with a negative charge introduced at position 551, NBD dimerization is likely prohibited as the result of simple electrostatic repulsion. To test the hypothesis, we mutated G551 to S, K, and E, respectively. With a neutral (G551S) or cationic (G551K) side chain at residue 551, the channels respond to ATP in a manner similar to that of WT-CFTR. ATP serves as a pure stimulatory ligand, and the current drops to the baseline upon ATP removal (Fig. 6, A and B). In contrast, G551E-CFTR channels behave just like G551D-CFTR (Fig. 6 C), suggesting that an anionic side chain at residue 551 is required to confer this inhibitory action to site 2. Collectively, we modified the gating scheme originally proposed for WT-CFTR (Jih et al., 2012) by eliminating NBD-dimerized states (Fig. 6 D) to explain G551D-induced gating defects.

But, is the remaining four-state scheme (Fig. 6 D) sufficient to explain G551D-CFTR gating? Note there are two open states ("monoliganded" and "biliganded") in this simple equilibrium gating model. Interestingly, we noticed that the raw current traces in Van Goor et al. (2009) indeed suggest the existence of at least two different opening events for G551D-CFTR in the presence of VX-770. To further test this idea, we recorded microscopic currents of G551D-CFTR in the presence of 20 μM ATP (Fig. 7 A), a concentration meant to keep a minimum occupancy of site 2 but at the same time an occupied site 1. In other words, by lowering [ATP], we intended to keep the channel in monoliganded states. Fig. 7 A shows samples of raw current traces of G551D-CFTR at 20 μM ATP. There still appears to be two populations of opening events distinguished by their open times. Indeed, the open time histogram (Fig. 7 B) confirms two different components ($\tau_1 = 57$ ms, $\tau_2 = 436$ ms). Similar observations were made for G551D/Y1219G-CFTR, in which 20 μM ATP is expected to bear negligible ATP occupancy at site 2 (Fig. 7, C and D). Thus, even for monoliganded G551D channels, there exist two distinct open states, an observation which is inconsistent with the modified model depicted in Fig. 6 D. Possible kinetic mechanisms will be discussed.

DISCUSSION

More than two decades of biophysical studies of CFTR gating have led us to a model (Jih et al., 2012) that exemplifies the critical role of site 2 in ATP-induced NBD dimerization and a probabilistic relationship between NBD dimerization and channel gating (Fig. 6 D; but cf.

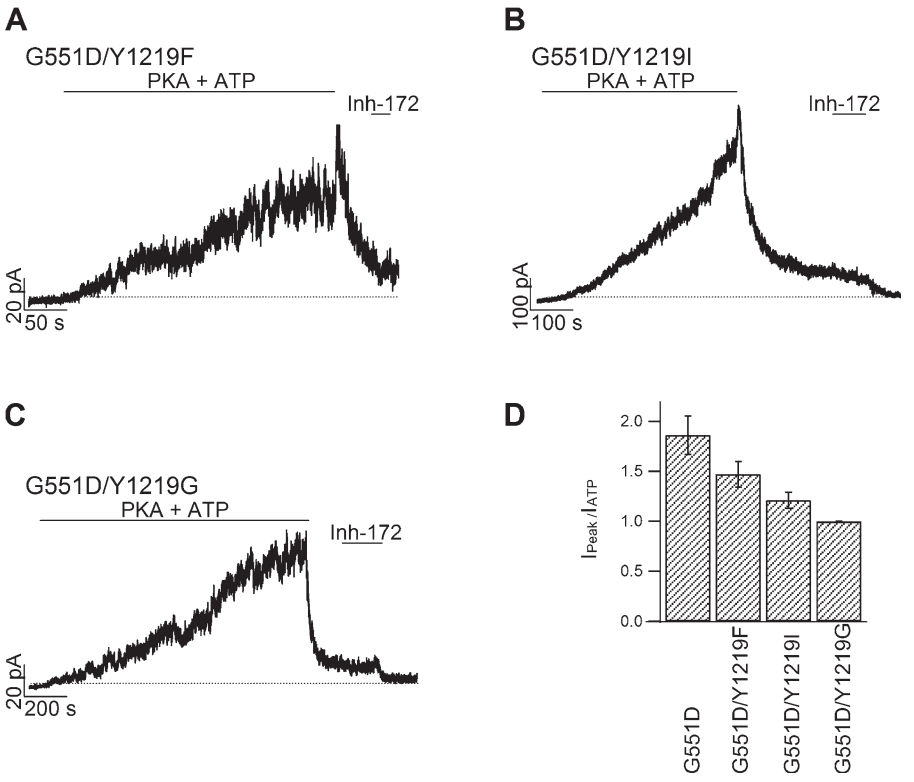

Figure 4. Effects of mutations at Y1219 on the response of G551D-CFTR to ATP washout. (A–C) Real-time current traces in response to ATP removal for G551D/Y1219F (A), G551D/Y1219I (B), and G551D/Y1219G (C). (D) Summary of the ratios between the peak current after ATP washout (I_{PEAK}) and the steady-state current before ATP removal (I_{ATP}) for G551D and its variants. Mean ± SEM is shown.

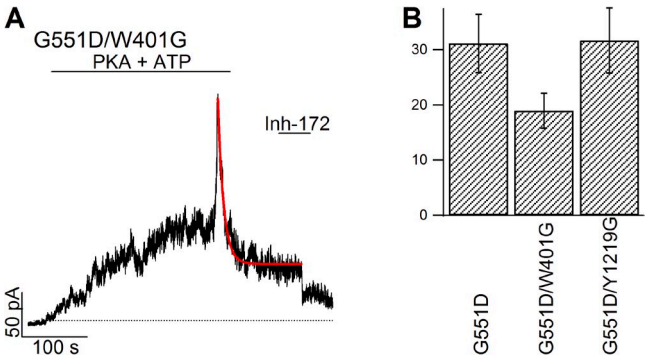

Figure 5. Characterization of the slow current decay in G551D-CFTR. (A) Acceleration of the slow-phase current decay by the W401G mutation. A continuous recording demonstrates an unequivocal biphasic response upon ATP washout for G551D/W401G-CFTR. The current decay phase was fitted with a single exponential function (red line), yielding a time constant of 17.6 s, which is significantly shorter than that of G551D-CFTR ($P < 0.05$). (B) Summary of time constant of the slow current decay in different mutants. 31.1 ± 5.3 s ($n = 12$) for G551D-CFTR, 19.0 ± 3.2 s ($n = 8$) for G551D/W401G-CFTR, and 31.7 ± 5.9 s ($n = 12$) for G551D/Y1219G-CFTR. Mean ± SEM is shown.

Csanády et al., 2010). The data presented in the current manuscript support the notion that this functionally important site 2 is converted to an inhibitory site in G551D-CFTR, a conclusion independent of any kinetic model for CFTR gating. The chemical basis for this peculiar conversion is likely caused by a simple electrostatic repulsion between two negative charges inherent, respectively, in the γ-phosphate of ATP and the carboxyl side chain of aspartate at position 551 (Fig. 6). Once we accept this chemical mechanism that is also supported by recent computational work (Xu et al., 2014), it seems safe to discount any role of NBD dimerization in G551D-CFTR gating. We therefore remove the NBD-dimerized states in Fig. 6 D for the G551D mutant (compare Bompadre et al., 2007). The scheme can be further simplified by eliminating the hydrolytic pathway for channel closure because NBD dimerization is a prerequisite for effective ATP hydrolysis in ABC proteins including CFTR (Li et al., 1996; Kidd et al., 2004; Cheung et al., 2008). However, the remaining four-state scheme (Fig. 6 D) underpinning the gating mechanism for G551D-CFTR may still not suffice for the following reasons.

First, it obviously fails to explain the slow decay phase seen in both WT- and G551D-CFTR (Fig. 2). The simplest explanation for this slow current decay upon ATP removal is that the ATP dissociation from site 1 (presumably after a disengagement of the NBD1 head and the NBD2 tail) poses a negative impact on channel gating as suggested by the raw current trace in Fig. 2 C. Of note, the role of site 1 in CFTR gating has been somewhat controversial (Powe et al., 2002; Basso et al., 2003; Csanády et al., 2010), but is nevertheless generally accepted to be less important than site 2. Our data demonstrates that in the absence of a functional site 2, whether site 1 is occupied by ATP does make a difference in channel gating. To explain this piece of data, one will have to expand the scheme beyond the scope of this work. We thus decided to refrain ourselves from further discussion.

Second, this four-state scheme cannot account for two distinct open states observed when the experimental

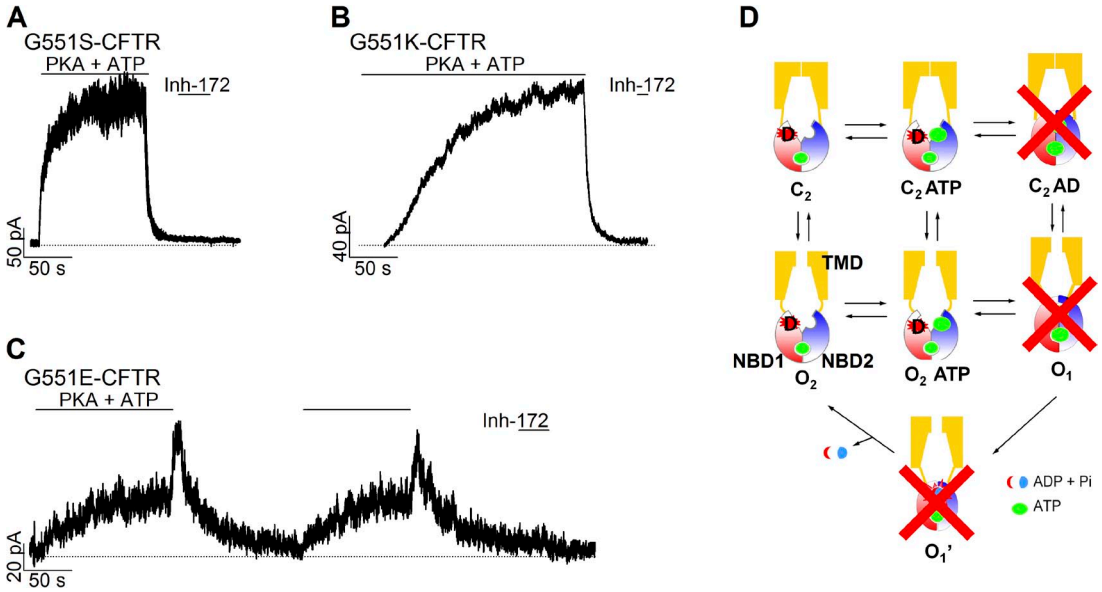

Figure 6. A negative charge at position 551 is needed to confer the inhibitory effect of ATP on CFTR gating. (A–C) Responses to ATP withdrawal in different G551 mutants: G551S (A), G551K (B), and G551E (C). (D) A modified gating model with NBD-dimerized states crossed out for G551D-CFTR. CFTR's TMDs and NBDs are marked in one of the cartoon representations of the CFTR protein: NBD1 in red and NBD2 in blue. "D" in the red star depicts the location of G551D in the tail subdomain of NBD1. As marked, the green circles denote the ligand ATP.

conditions are designed to assess the gating behavior of monoliganded G551D-CFTR (Fig. 7). But, once this simple equilibrium gating model is rejected, how can we explain kinetically the inhibitory effect of ATP binding on site 2 of G551D-CFTR channels? Although we found that none of the existing gating models published so far in the field (Csanády et al., 2010; Kirk and Wang, 2011; Jih and Hwang, 2012) provide a satisfactory explanation for these microscopic kinetic data, the idea of an energetic coupling between opening/closing of the gate and association/dissociation of the NBDs does offer a possible solution. This energetic coupling between NBD dimerization and gate opening predicts that the O_2 state in the G551D-CFTR should also favor dimerization of its NBDs, which, if it occurs, likely will proceed very slowly without a bound ATP molecule in site 2. By simply adding another open state (O_0) depicting an open channel conformation with a dimerized NBDs but an empty site 2, we can provide a tentative explanation for not only microscopic data shown in Fig. 7, but also ATP-dependent inhibition of macroscopic G551D-CFTR currents.

First, this slight modification of the four-state scheme is consistent with the observation of two distinct populations of the opening events (O_2 and O_0) when site 2 is kept vacant. Of note, the O_0 state is the equivalent state of the one with a dimerized NBDs (or O_1) that has been eliminated in Fig. 6 D. Both O_0 and O_1 represent NBD-dimerized states with an open gate; the only difference is the presence of ATP in site 2 or not. As the O_0 state resembles the stable O_1 state, this open state is expected to assume a longer open time. In contrast, the O_2 state is known to be short lived (Csanády et al., 2010; Jih et al., 2012). Once the O_0 state is added to the scheme, the inhibitory action of ATP in G551D-CFTR can be explained by a trapping of the channel in the C_2 ATP state in the presence of millimolar ATP; the removal of ATP allows the channel to travel to the more stable O_0 state, causing an increase of the current. Although appending additional states to the scheme depicted in Fig. 6 D may satisfactorily explain our microscopic and macroscopic data, we realize that this may not be the only solution. Certainly more extensive studies are needed to address these issues and to investigate whether this speculative mechanism may bear any relevance to WT-CFTR gating.

As described in the Results, this inhibitory action of ATP on G551D-CFTR is also present in the absence of VX-770 (Fig. 3 C). The microscopic nature of G551D-CFTR

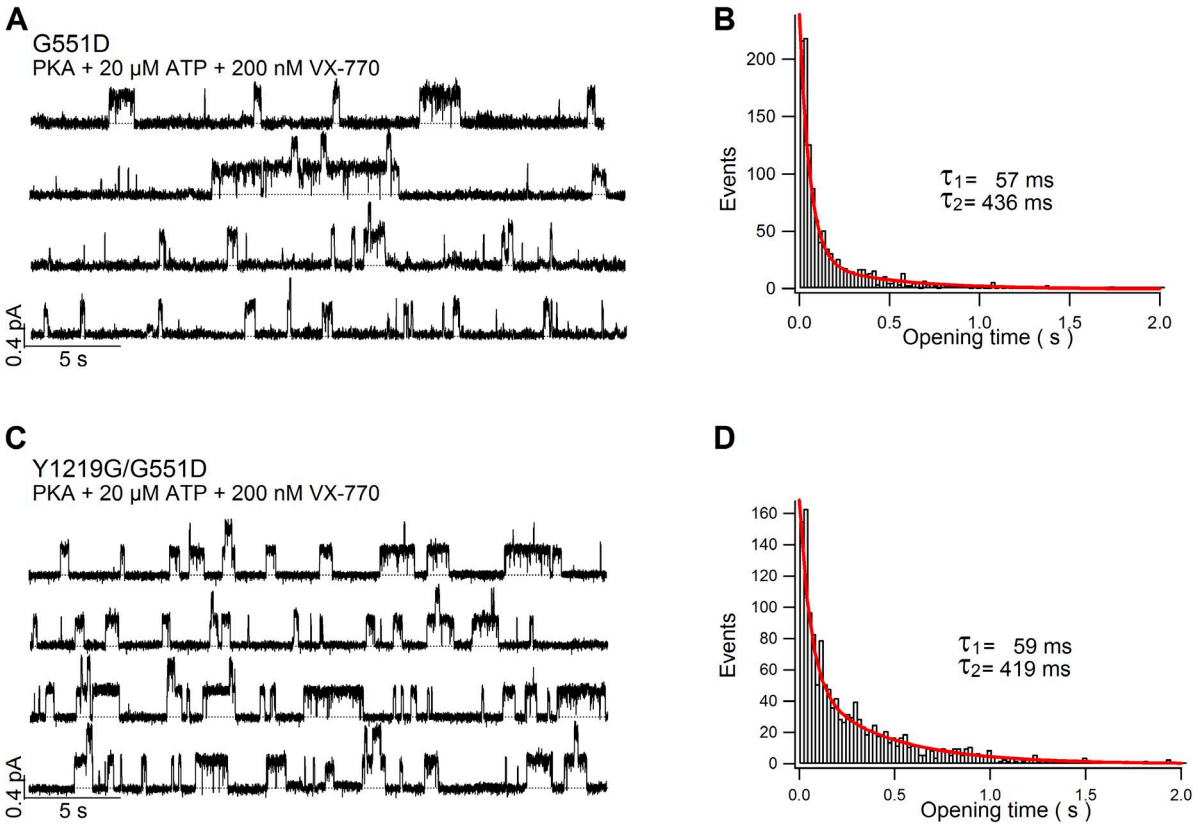

Figure 7. Two populations of opening events differentiated by distinct open time. (A) Single-channel recording of G551D-CFTR in the presence of 20 μM ATP. (B) Open time histogram for G551D-CFTR. A total of 1,665 events collected from four different patches were analyzed. The red line marks curve fit using a double exponential function. (C) Single-channel recording of G551D/Y1219G-CFTR in the presence of 20 μM ATP. (D) Open time histogram for G551D/Y1219G-CFTR. A total of 1,502 events collected from four separate patches were analyzed. The red line marks curve fit using a double exponential function.

currents in the absence of VX-770 may have prevented an unequivocal resolution of biphasic changes of the current upon ATP removal, thus accounting for previous overlook of this intriguing phenomenon (Bompadre et al., 2007). However, it puzzles us as to why the inverse [ATP] dependence of G551D-CFTR (Fig. 3 C) was never reported in the past, although a recent study (Xu et al., 2014) did characterize this mutant CFTR at different [ATP]. We noted that in Xu et al. (2014), 0.1, 1, and 5 mM [ATP] were tested on G551D-CFTR in the absence of VX-770. As 0.1 mM [ATP] may be sufficient to occupy site 2 to a significant extent, we suspect that the difference in activity of this mutant channel at these tested concentrations of ATP may be too small to be detected.

In addition to offering some more insights into the gating mechanism of CFTR, our work could also shed light on possible new strategies for developing novel therapies for patients carrying the G551D mutation. Although VX-770 has been approved by the FDA for the treatment of CF patients carrying the G551D mutation, it may be still a long way to a complete cure. Using cAMP-dependent sweating as an in vivo measurement for CFTR activity, Char et al. (2014) estimated VX-770–rectified G551D-CFTR function to be ∼5% of the WT mean. Thus, a further improvement of G551D-CFTR activity with compounds that can complement the action of VX-770 is expected to benefit these CF patients currently taking Ivacaftor. Our demonstration of a significant inhibition of G551D-CFTR by ATP opens the door for a new strategy of drug development. By designing reagents that can compete off ATP binding to site 2, we expect a doubling of G551D-CFTR function by eliminating this inhibitory action of ATP. As the high-resolution crystal structures of CFTR's two NBDs are now solved (Patrick and Thomas, 2012), in silico drug design may soon become a reality for at least a subset of patients with CF.

We thank Cindy Chu and Shenghui Hu for their technical assistance and Dr. Robert Bridges for providing VX-770. We also thank Yong-Cheng Ye and Joseph Huang for their efforts in carrying out some pilot experiments.

Wen-Ying Lin is a recipient of a scholarship (no. 102-Y-A-001) from the Taipei Veterans General Hospital–National Yang-Ming University Excellent Physician Scientists Cultivation Program in Taiwan. This work is supported by R01DK55835 from the National Institutes of Health and a grant (Hwang13P0) from the Cystic Fibrosis Foundation (to T.-C. Hwang).

The authors declare no competing financial interests.

Merritt C. Maduke served as editor.

Submitted: 16 June 2014
Accepted: 15 August 2014

REFERENCES

Accurso, F.J., S.M. Rowe, J.P. Clancy, M.P. Boyle, J.M. Dunitz, P.R. Durie, S.D. Sagel, D.B. Hornick, M.W. Konstan, S.H. Donaldson, et al. 2010. Effect of VX-770 in persons with cystic fibrosis and the G551D-CFTR mutation. *N. Engl. J. Med.* 363:1991–2003. http://dx.doi.org/10.1056/NEJMoa0909825

Aleksandrov, L., A. Mengos, X. Chang, A. Aleksandrov, and J.R. Riordan. 2001. Differential interactions of nucleotides at the two nucleotide binding domains of the cystic fibrosis transmembrane conductance regulator. *J. Biol. Chem.* 276:12918–12923. http://dx.doi.org/10.1074/jbc.M100515200

Aleksandrov, L., A.A. Aleksandrov, X.-B. Chang, and J.R. Riordan. 2002. The first nucleotide binding domain of cystic fibrosis transmembrane conductance regulator is a site of stable nucleotide interaction, whereas the second is a site of rapid turnover. *J. Biol. Chem.* 277:15419–15425. http://dx.doi.org/10.1074/jbc.M111713200

Basso, C., P. Vergani, A.C. Nairn, and D.C. Gadsby. 2003. Prolonged nonhydrolytic interaction of nucleotide with CFTR's NH_2-terminal nucleotide binding domain and its role in channel gating. *J. Gen. Physiol.* 122:333–348. http://dx.doi.org/10.1085/jgp.200308798

Bear, C.E., C.H. Li, N. Kartner, R.J. Bridges, T.J. Jensen, M. Ramjeesingh, and J.R. Riordan. 1992. Purification and functional reconstitution of the cystic fibrosis transmembrane conductance regulator (CFTR). *Cell.* 68:809–818. http://dx.doi.org/10.1016/0092-8674(92)90155-6

Bompadre, S.G., T. Ai, J.H. Cho, X. Wang, Y. Sohma, M. Li, and T.-C. Hwang. 2005. CFTR gating I: Characterization of the ATP-dependent gating of a phosphorylation-independent CFTR channel (ΔR-CFTR). *J. Gen. Physiol.* 125:361–375. http://dx.doi.org/10.1085/jgp.200409227

Bompadre, S.G., Y. Sohma, M. Li, and T.-C. Hwang. 2007. G551D and G1349D, two CF-associated mutations in the signature sequences of CFTR, exhibit distinct gating defects. *J. Gen. Physiol.* 129:285–298. http://dx.doi.org/10.1085/jgp.200609667

Char, J.E., M.H. Wolfe, H.J. Cho, I.-H. Park, J.H. Jeong, E. Frisbee, C. Dunn, Z. Davies, C. Milla, R.B. Moss, et al. 2014. A little CFTR goes a long way: CFTR-dependent sweat secretion from G551D and R117H-5T cystic fibrosis subjects taking ivacaftor. *PLoS ONE.* 9:e88564. http://dx.doi.org/10.1371/journal.pone.0088564

Cheung, J.C., P. Kim Chiaw, S. Pasyk, and C.E. Bear. 2008. Molecular basis for the ATPase activity of CFTR. *Arch. Biochem. Biophys.* 476:95–100. http://dx.doi.org/10.1016/j.abb.2008.03.033

Csanády, L., P. Vergani, and D.C. Gadsby. 2010. Strict coupling between CFTR's catalytic cycle and gating of its Cl^- ion pore revealed by distributions of open channel burst durations. *Proc. Natl. Acad. Sci. USA.* 107:1241–1246. http://dx.doi.org/10.1073/pnas.0911061107

Gregory, R.J., D.P. Rich, S.H. Cheng, D.W. Souza, S. Paul, P. Manavalan, M.P. Anderson, M.J. Welsh, and A.E. Smith. 1991. Maturation and function of cystic fibrosis transmembrane conductance regulator variants bearing mutations in putative nucleotide-binding domains 1 and 2. *Mol. Cell. Biol.* 11:3886–3893.

Hwang, T.-C., and D.N. Sheppard. 2009. Gating of the CFTR Cl^- channel by ATP-driven nucleotide-binding domain dimerisation. *J. Physiol.* 587:2151–2161. http://dx.doi.org/10.1113/jphysiol.2009.171595

Jih, K.-Y., and T.-C. Hwang. 2012. Nonequilibrium gating of CFTR on an equilibrium theme. *Physiology (Bethesda).* 27:351–361. http://dx.doi.org/10.1152/physiol.00026.2012

Jih, K.-Y., and T.-C. Hwang. 2013. Vx-770 potentiates CFTR function by promoting decoupling between the gating cycle and ATP hydrolysis cycle. *Proc. Natl. Acad. Sci. USA.* 110:4404–4409. http://dx.doi.org/10.1073/pnas.1215982110

Jih, K.-Y., Y. Sohma, and T.-C. Hwang. 2012. Nonintegral stoichiometry in CFTR gating revealed by a pore-lining mutation. *J. Gen. Physiol.* 140:347–359. http://dx.doi.org/10.1085/jgp.201210834

Jones, P.M., and A.M. George. 2007. Nucleotide-dependent allostery within the ABC transporter ATP-binding cassette: a computational study of the MJ0796 dimer. *J. Biol. Chem.* 282:22793–22803. http://dx.doi.org/10.1074/jbc.M700809200

Kidd, J.F., M. Ramjeesingh, F. Stratford, L.J. Huan, and C.E. Bear. 2004. A heteromeric complex of the two nucleotide binding

domains of cystic fibrosis transmembrane conductance regulator (CFTR) mediates ATPase activity. *J. Biol. Chem.* 279:41664–41669. http://dx.doi.org/10.1074/jbc.M407666200

Kirk, K.L., and W. Wang. 2011. A unified view of cystic fibrosis transmembrane conductance regulator (CFTR) gating: combining the allosterism of a ligand-gated channel with the enzymatic activity of an ATP-binding cassette (ABC) transporter. *J. Biol. Chem.* 286:12813–12819. http://dx.doi.org/10.1074/jbc.R111.219634

Kopeikin, Z., Y. Sohma, M. Li, and T.-C. Hwang. 2010. On the mechanism of CFTR inhibition by a thiazolidinone derivative. *J. Gen. Physiol.* 136:659–671. http://dx.doi.org/10.1085/jgp.201010518

Lewis, H.A., S.G. Buchanan, S.K. Burley, K. Conners, M. Dickey, M. Dorwart, R. Fowler, X. Gao, W.B. Guggino, W.A. Hendrickson, et al. 2004. Structure of nucleotide-binding domain 1 of the cystic fibrosis transmembrane conductance regulator. *EMBO J.* 23:282–293. http://dx.doi.org/10.1038/sj.emboj.7600040

Li, C., M. Ramjeesingh, W. Wang, E. Garami, M. Hewryk, D. Lee, J.M. Rommens, K. Galley, and C.E. Bear. 1996. ATPase activity of the cystic fibrosis transmembrane conductance regulator. *J. Biol. Chem.* 271:28463–28468. http://dx.doi.org/10.1074/jbc.271.45.28463

Miki, H., Z. Zhou, M. Li, T.-C. Hwang, and S.G. Bompadre. 2010. Potentiation of disease-associated cystic fibrosis transmembrane conductance regulator mutants by hydrolyzable ATP analogs. *J. Biol. Chem.* 285:19967–19975. http://dx.doi.org/10.1074/jbc.M109.092684

Ostedgaard, L.S., O. Baldursson, and M.J. Welsh. 2001. Regulation of the cystic fibrosis transmembrane conductance regulator Cl^- channel by its R domain. *J. Biol. Chem.* 276:7689–7692. http://dx.doi.org/10.1074/jbc.R100001200

Patrick, A.E., and P.J. Thomas. 2012. Development of CFTR structure. *Front. Pharmacol.* 3:162. http://dx.doi.org/10.3389/fphar.2012.00162

Powe, A.C. Jr., L. Al-Nakkash, M. Li, and T.-C. Hwang. 2002. Mutation of Walker-A lysine 464 in cystic fibrosis transmembrane conductance regulator reveals functional interaction between its nucleotide-binding domains. *J. Physiol.* 539:333–346. http://dx.doi.org/10.1113/jphysiol.2001.013162

Quinton, P.M., and M.M. Reddy. 1991. Regulation of absorption in the human sweat duct. *Adv. Exp. Med. Biol.* 290:159–172. http://dx.doi.org/10.1007/978-1-4684-5934-0_17

Ramsey, B.W., J. Davies, N.G. McElvaney, E. Tullis, S.C. Bell, P. Dřevínek, M. Griese, E.F. McKone, C.E. Wainwright, M.W. Konstan, et al. VX08-770-102 Study Group. 2011. A CFTR potentiator in patients with cystic fibrosis and the G551D mutation. *N. Engl. J. Med.* 365:1663–1672. http://dx.doi.org/10.1056/NEJMoa1105185

Ren, X.-Q., T. Furukawa, M. Haraguchi, T. Sumizawa, S. Aoki, M. Kobayashi, and S. Akiyama. 2004. Function of the ABC signature sequences in the human multidrug resistance protein 1. *Mol. Pharmacol.* 65:1536–1542. http://dx.doi.org/10.1124/mol.65.6.1536

Riordan, J.R., J.M. Rommens, B. Kerem, N. Alon, R. Rozmahel, Z. Grzelczak, J. Zielenski, S. Lok, N. Plavsic, J.L. Chou, et al. 1989. Identification of the cystic fibrosis gene: cloning and characterization of complementary DNA. *Science.* 245:1066–1073. http://dx.doi.org/10.1126/science.2475911

Rowe, S.M., S. Miller, and E.J. Sorscher. 2005. Mechanisms of disease: Cystic fibrosis. *N. Engl. J. Med.* 352:1992–2001. http://dx.doi.org/10.1056/NEJMra043184

Smith, P.C., N. Karpowich, L. Millen, J.E. Moody, J. Rosen, P.J. Thomas, and J.F. Hunt. 2002. ATP binding to the motor domain from an ABC transporter drives formation of a nucleotide sandwich dimer. *Mol. Cell.* 10:139–149. http://dx.doi.org/10.1016/S1097-2765(02)00576-2

Stratford, F.L.L., M. Ramjeesingh, J.C. Cheung, L.-J. Huan, and C.E. Bear. 2007. The Walker B motif of the second nucleotide-binding domain (NBD2) of CFTR plays a key role in ATPase activity by the NBD1-NBD2 heterodimer. *Biochem. J.* 401:581–586. http://dx.doi.org/10.1042/BJ20060968

Szabó, K., G. Szakács, T. Hegeds, and B. Sarkadi. 1999. Nucleotide occlusion in the human cystic fibrosis transmembrane conductance regulator. Different patterns in the two nucleotide binding domains. *J. Biol. Chem.* 274:12209–12212. http://dx.doi.org/10.1074/jbc.274.18.12209

Szentpétery, Z., A. Kern, K. Liliom, B. Sarkadi, A. Váradi, and E. Bakos. 2004a. The role of the conserved glycines of ATP-binding cassette signature motifs of MRP1 in the communication between the substrate-binding site and the catalytic centers. *J. Biol. Chem.* 279:41670–41678. http://dx.doi.org/10.1074/jbc.M406484200

Szentpétery, Z., B. Sarkadi, E. Bakos, and A. Váradi. 2004b. Functional studies on the MRP1 multidrug transporter: characterization of ABC-signature mutant variants. *Anticancer Res.* 24:449–455.

Tsai, M.-F., H. Shimizu, Y. Sohma, M. Li, and T.-C. Hwang. 2009. State-dependent modulation of CFTR gating by pyrophosphate. *J. Gen. Physiol.* 133:405–419. http://dx.doi.org/10.1085/jgp.200810186

Tsai, M.-F., M. Li, and T.-C. Hwang. 2010. Stable ATP binding mediated by a partial NBD dimer of the CFTR chloride channel. *J. Gen. Physiol.* 135:399–414. http://dx.doi.org/10.1085/jgp.201010399

Van Goor, F., S. Hadida, P.D. Grootenhuis, B. Burton, D. Cao, T. Neuberger, A. Turnbull, A. Singh, J. Joubran, A. Hazlewood, et al. 2009. Rescue of CF airway epithelial cell function in vitro by a CFTR potentiator, VX-770. *Proc. Natl. Acad. Sci. USA.* 106:18825–18830. http://dx.doi.org/10.1073/pnas.0904709106

Vergani, P., A.C. Nairn, and D.C. Gadsby. 2003. On the mechanism of MgATP-dependent gating of CFTR Cl^- channels. *J. Gen. Physiol.* 121:17–36. http://dx.doi.org/10.1085/jgp.20028673

Vergani, P., S.W. Lockless, A.C. Nairn, and D.C. Gadsby. 2005. CFTR channel opening by ATP-driven tight dimerization of its nucleotide-binding domains. *Nature.* 433:876–880. http://dx.doi.org/10.1038/nature03313

Xu, Z., L.S. Pissarra, C.M. Farinha, J. Liu, Z. Cai, P.H. Thibodeau, M.D. Amaral, and D.N. Sheppard. 2014. Revertant mutants modify, but do not rescue, the gating defect of the cystic fibrosis mutant G551D-CFTR. *J. Physiol.* 592:1931–1947.

Zhou, Z., X. Wang, H.-Y. Liu, X. Zou, M. Li, and T.-C. Hwang. 2006. The two ATP binding sites of cystic fibrosis transmembrane conductance regulator (CFTR) play distinct roles in gating kinetics and energetics. *J. Gen. Physiol.* 128:413–422. http://dx.doi.org/10.1085/jgp.200609622

Zielenski, J., and L.C. Tsui. 1995. Cystic fibrosis: genotypic and phenotypic variations. *Annu. Rev. Genet.* 29:777–807. http://dx.doi.org/10.1146/annurev.ge.29.120195.004021